ICANS-XV
15th Meeting of the International Collaboration on Advanced Neutron Sources
November 6-9, 2000
Tsukuba, Japan

19.1
Shielding Design Study for the JAERI/KEK Spallation Neutron Source

Fujio Maekawa*, Makoto Teshigawara, Chikara Konno, Yujiro Ikeda and Noboru Watanabe

Japan Atomic Energy Research Institute, Tokai 319-1195, Japan
* fujio@fnshp.tokai.jaeri.go.jp

Abstract

Shielding design for the JAERI/KEK spallation neutron source was studied. Bulk shielding characteristics and optimization of a beam shutter were investigated by using Monte Carlo calculation codes NMTC/JAM and MCNP with LA-150 neutron cross section library. The following remarks were derived. (1) Neutron dose outside of the concrete shield at 6.6 m from the center is ~ 10 μSv/hr regardless of angles with respect to the proton beam axis. The neutron dose can be reduced more than a factor of 30 by adding natural boron of 5 wt% in the concrete. (2) When a beam shutter position just outside the void vessel and the shutter length of 2 m are assumed, a shutter made of copper (1.7 m) with polyethylene (0.3 m) is the optimum in terms of shielding performance as well as cost merit. A shutter made of tungsten is not so effective. (3) Further studies are needed for optimization of beam shutter position.

1. Introduction

It has already been recognized that the neutronic calculation on neutron beam line shield is one of the most important but difficult issues in the design study of intense spallation neutron sources. From a view point of shielding calculation, the spallation neutron source has rather difficult complexity in the three-dimensional TMRA including many small parts, strongly angle-dependent distributions of high-energy source neutron produced by proton-induced spallation reactions, and many neutron beam lines penetrating through a very thick bulk shield. To investigate adequate shielding, i.e., sufficient but not too much, we have started shielding design calculations for the JAERI/KEK spallation neutron source. This paper deals with the following two topics: (1) bulk shielding calculations for a shield consisting of cast iron (5 m) and concrete (1 m), and (2) optimization of a beam shutter configuration.

2. Calculation Models and Tools

According to the latest design of the JAERI/KEK spallation neutron source, the following proton beam conditions were assumed: 3 GeV energy, 1 MW power, and rectangular beam size of 130 mm (horizontal) by 50 mm (vertical). Figure 1 illustrates a three-dimensional calculation model for inside of the void vessel. A mercury target, a liquid hydrogen moderator on the target,

a light water moderator and a liquid hydrogen moderator under the target, pre-moderators and a lead reflector form a target-moderator-reflector assembly (TMRA) of 0.6 m in radius and 0.6 m in half-height. The TMRA is surrounded by a shield made of cast iron (7.3 g/cm^3, 90 % in volume) with cooling water (10 % in volume). Dimensions of the void vessel are 1.5 m in radius and 1.5 m in half-height. Seven and thirteen neutron beam lines above and below the target, respectively, are considered in the model. Each beam line has a square section of 100 mm by 100 mm. For beam line shielding calculations hereafter, the most forward directed beam line at 32.5 degrees with respect to the proton beam axis was considered because it was the most severe case in view of shielding. A distance between the center of the target and the lower end of the beam line is 90 mm (see Fig. 1 (b)).

For particle transport calculations, three Monte Carlo simulation codes, the NMTC/JAM code (version 1.00) [1], the MCNPX code (version 2.1.5) [2] and the MCNP-4C code [3] were employed. The LA-150 [4] neutron transport cross section library was used for the MCNP calculations.

3. Bulk Shielding Calculation

3.1 Source Term Calculation

The bulk shielding calculation took two steps: a source term calculation and bulk shielding calculations. For the source term calculation, the TMRA model in Fig. 1 without the surrounding cast iron shield, i.e., the cylindrical part of 0.6 m in radius and 0.6 m in half-height, was used. Spectral fluxes of neutrons leaking from the TMRA were scored by a very large spherical surface tally that centered the TMRA. To consider the anisotropy of neutron production, the surface was divided into 12 segments to score neutrons leaking toward every 15 degrees with respect to the proton beam axis. The NMTC/JAM code and the MCNP-4C code with

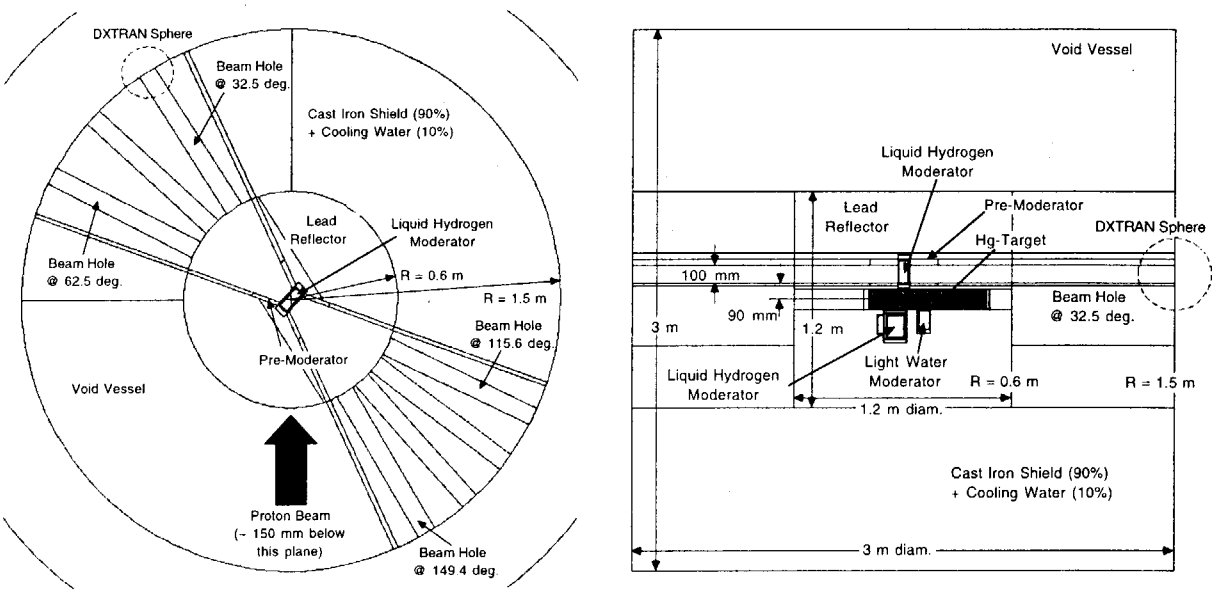

Fig. 1 Calculation model for inside of the void vessel.

LA-150 were used above and below 150 MeV, respectively.

Figure 2 shows calculated neutron spectra for four angle ranges. Very strong angle-dependence of neutron fluxes is found in the high energy part of spectra above 10 MeV. Most of neutrons are in an energy range below 10 MeV, and the angle-dependence is not so remarkable for the low-energy neutrons.

3.2 Bulk Shielding Calculation

The second step was the bulk shielding calculation with a one-dimensional spherical model shown in Fig. 3. The TMRA was represented as a point source at the center that emitted source neutrons having a spectrum for one of the 12 angle ranges. The central sphere within 0.6 m in radius was a void region, and it was surrounded by a cast iron shield (7.3 g/cm^3) of 5 m thickness and a concrete shield (2.1 g/cm^3) of 1 m thickness. Calculations were repeated for 12 times by changing the angle-dependent source neutron spectrum. The MCNPX code was used with the LA-150 library. The weight window technique was adopted for variance reduction with choosing weight window parameters carefully.

The two-step calculation overestimates the results due to the following two reasons. (1) All source neutrons are emitted to the direction of μ (cos θ) = 1 in the two-step calculation

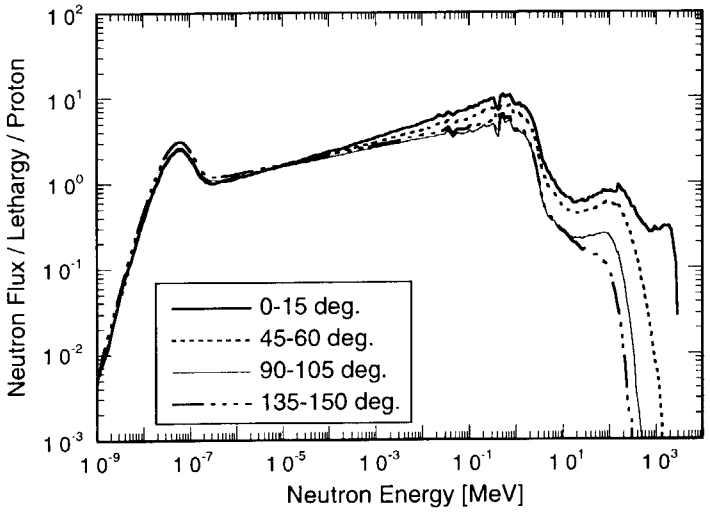

Fig. 2 Spectral fluxes of neutrons leaking from the TMRA for four angle ranges.

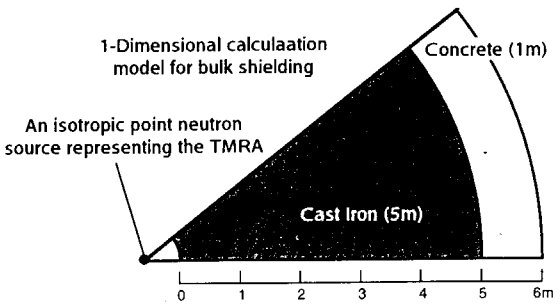

Fig. 3 One-dimensional spherical model for the bulk shielding calculations.

although neutrons have various μ values ranging from 0 to 1 in the real situation. Neutrons going to the μ = 1 direction are the most likely to penetrate the shield. (2) In the two-step calculation, when a neutron is scattered in the iron region and returns to the void region, the neutron reenter to the opposite side of the iron shield immiditely. In the real case, such neutron enters into the lead reflector to be slowed down and/or absorbed.

Calculated neutron spectra for several shield thicknesses for the 0-15 degree neutron source are shown in Fig. 4. In the iron shield up to 5 m, neutron fluxes above 1 MeV decrease constantly by about two orders of magnitude for every 1 m thicknesses while those below 1 MeV do not attenuate as effective as the high energy part. In the concrete shield, on the contrary, neutron fluxes in an energy range from 0.4 eV to 1 MeV attenuate drastically, i.e., about 10 orders of magnitude in 1 m, and slowed down neutrons accumulate in the thermal energy region.

Figure 5 shows neutron dose distributions in the bulk shield for several angles. Neutron doses at the outside of the concrete shield are ~ 10 μSv/hr for the 1 MW operation regardless of

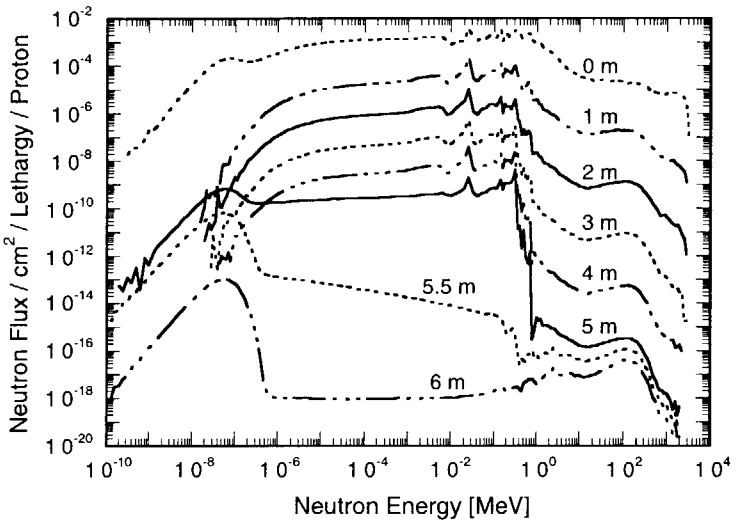

Fig. 4 Neutron spectra as a function of shield thickness calculated with the source neutrons for 0-15 degree angle ranges. Shield materials are cast iron up to 5 m and concrete from 5 m to 6 m.

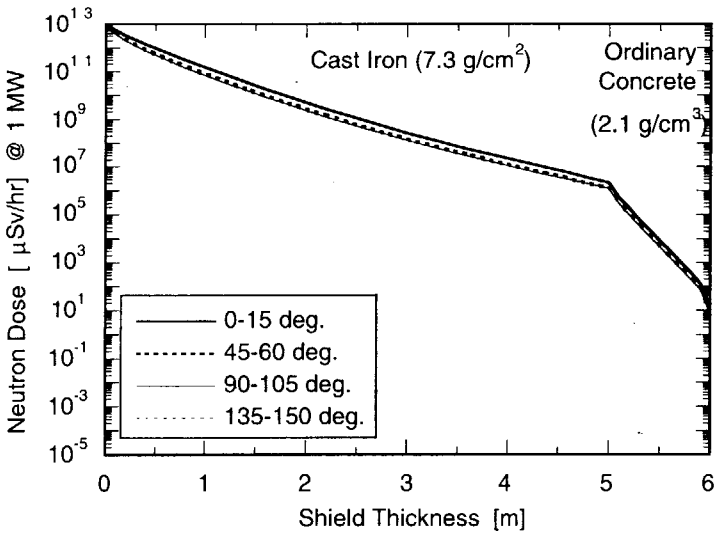

Fig. 5 Neutron dose distribution in the bulk shield.

the angle with respect to the proton beam axis. The angle-dependence of the neutron dose is not significant although high-energy source neutron fluxes have a strong angle-dependency as shown in Fig. 2. Neutrons below 1 MeV and thermal neutrons contribute dominantly to the neutron dose in the iron and the concrete shield, respectively. Most of these low-energy neutrons originate neutrons below 10 MeV in the source neutron flux in Fig. 2, and can penetrate the iron shield easily by the so-called window streaming due to the several minima of total cross section of iron between 20 keV to 400 keV. Therefore, the small angle-dependence of source neutron fluxes below 10 MeV is the reason for the little angle-dependence of the neutron dose.

3.3 Effect of Boron Doping in Concrete

From Fig. 4, it is expected that the neutron dose at the outside of the concrete shield can be reduced effectively by adding a thermal neutron absorbing material in the concrete. To demonstrate the idea, another series of calculations was conducted by adding 5 wt% of natural boron in the concrete with keeping the weight density of 2.1 g/cm^3. As indicated in Fig. 6, the effect of boron doping is remarkable. The neutron dose at the outside of the concrete is reduced to 0.3 μSv/hr for the most forward angle, and further less for other angles. In this case, an angle-dependence of the neutron dose is clearly seen. This indicates that thermal neutrons are absorbed by boron atoms almost entirely, and the high-energy neutrons above ~ 1 MeV contribute dominantly to the neutron dose.

4. Calculation for Beam Shutter

4.1 Source Term Calculation

Calculations for a beam shutter also took two steps, source term calculations and transmission calculations in shutters. For the source term calculation, the 3-D model shown in Fig. 1 was used. The NMTC/JAM code and the MCNP-4C code with LA-150 were used above and below 150 MeV, respectively.

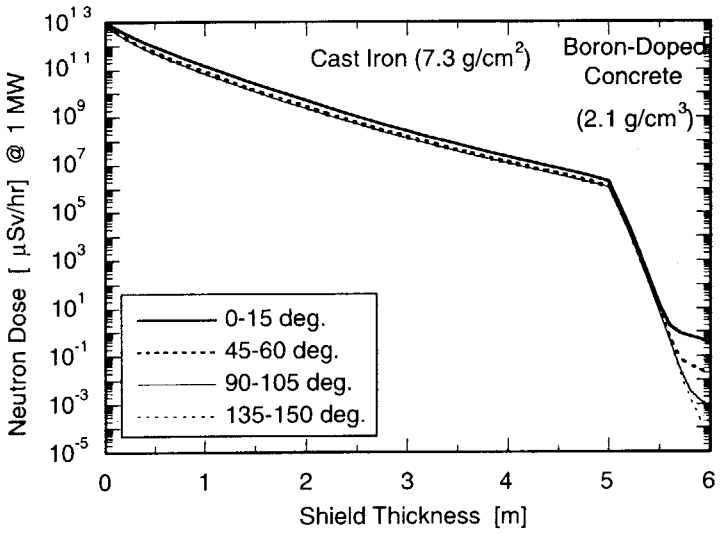

Fig. 6 Neutron dose distribution in the bulk shield with the boron-doped concrete.

Neutron flux intensities for the four beam lines at 32.5, 62.5, 115.6 and 149.4 degrees were calculated with the MCNP-4C code by putting a point detector at the exit of each beam line at 1.5 m from the center. Note that neutron spectra above 150 MeV could not be calculated because cross section data above 150 MeV which are needed for the point detectors were not available. As shown in Fig. 7, although angle-dependence of neutron flux intensity is not so significant below 10 MeV, neutron flux intensity around 100 MeV for the 32.5 degree is as nearly 10 times large as that for backward angles.

Neutron flux intensities were calculated in the same way by changing positions of the proton beam impingement by ± 16 mm for the 32.5 degree beam line. It was found from the results shown in Fig. 8 that the effects are not so significant, at most ± 20 %, even for high energy neutrons. This implies that the distance of 90 mm between the proton beam center to the bottom of the beam line is very effective to protect direct contributions from the target to the point detector. This fact was confirmed by analyzing the "score contributions by cell" given in the output file of MCNP calculation. Most of contributions to the point detector are from the moderator and materials in thin layers in just several centimeters surrounding the beam hole, but not from the target.

Finally, a source term for the second step was calculated. A DXTRAN sphere was placed at the exit of the 32.5 degree beam line at 1.5 from the center (see Fig. 1), and energy-angle dependent neutron current crossing a 100 mm x 100 mm plane at the exit was calculated.

4.2 Intensity of the Source Neutron flux Compared to That in Bulk Shield

When the intensity of the calculated source neutron fluxes are compared to the neutron flux in the bulk shield at the corresponding position, i.e., 1.5 m from the center, the former is not about 10 times larger than the latter (see Fig. 9). Hence, when a shutter that is located just outside of the void vessel and has a length of 2 m along the beam line is assumed, required performance for the shutter is to attenuate the neutron flux by ten times more than the attenuation in the surrounding cast iron of 2 m. Since high energy neutron fluxes attenuate by ~ 4.5 orders of magnitude in the cast iron of 2 m, attenuation of ~ 5.5 orders of magnitude is required for the shutter. To achieve this requirement, copper is a candidate material that has somewhat higher weight density of 8.93 g/cm^3.

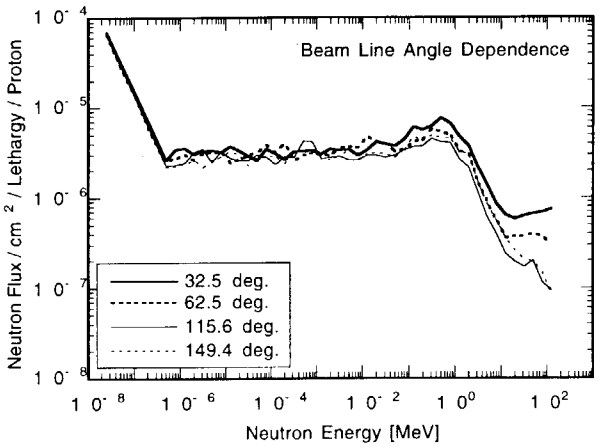

Fig. 7 Beam line angle dependence of neutron spectra at the exit of the four beam lines at 1.5 m from the center.

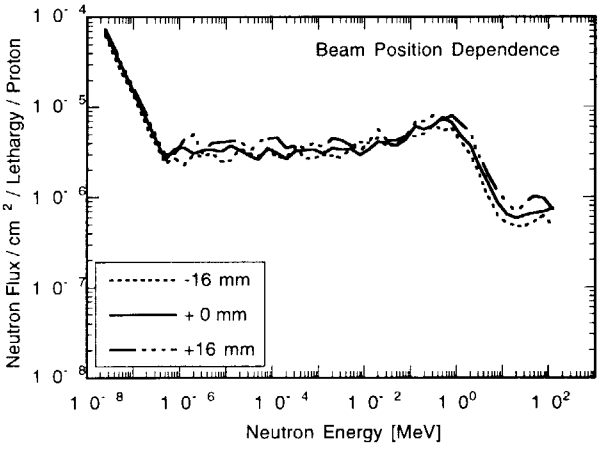

Fig. 8 Proton beam position dependence of neutron spectra at the exit of the 32.5 degree beam lines at 1.5 m from the center.

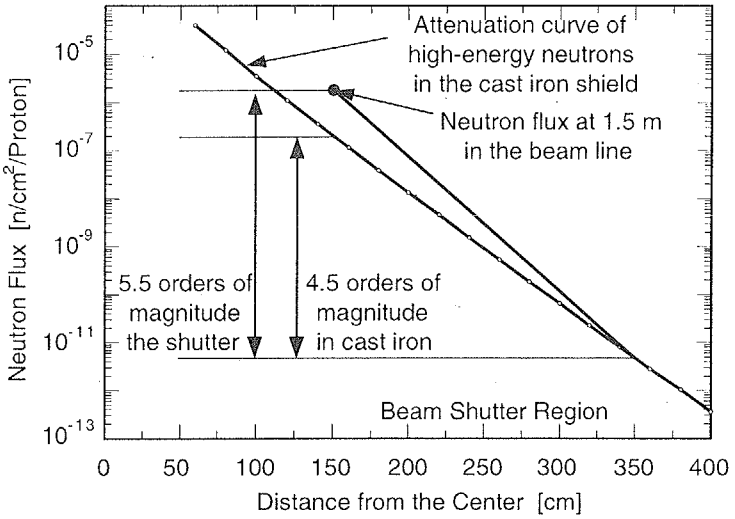

Fig. 9 Attenuation of neutron fluxes in the shutter and the bulk shield.

4.3 Optimization for Beam Shutter Configuration

An optimum beam shutter configuration was surveyed with the calculation model shown in Fig. 10. The shutter consists of a shielding plug made of a dense material at the head and an end plug made of a hydrogen contained material (concrete or polyethylene), and remaining spaces are filled with iron. Parameters changed for the optimization are the axial length (Z1), the lateral length (X) and the material of the shielding plug, and the axial length (Z2) and the material of the end plug. Neutron flux distributions in the shutter along the beam line and neutron dose at the point detector located at the exit of the concrete shield at 6.6 m from the center were calculated. Note that the calculations always underestimate neutron doses at the point detector because neutrons coming from everywhere other than the source plane of 100 x 100 mm and source neutrons above 150 MeV are not taken into account. The calculations are still effective for the optimization study to see relative changes of results when calculation parameters are changed.

Figure 11 shows total and high-energy (> 2.5 MeV) neutron flux distributions in the core and the side regions in four types of beam shutters (a) through (d). As for the shutter (a), the whole core region is made of tungsten (0.2 x 0.2 x 2.0 m). Although the high energy neutron flux attenuate rapidly up to 0.7 m in depth due to the high nucleus density of tungsten, the attenuation slows after 1 m. After the 0.8 m depth, the high-energy neutron flux in the side

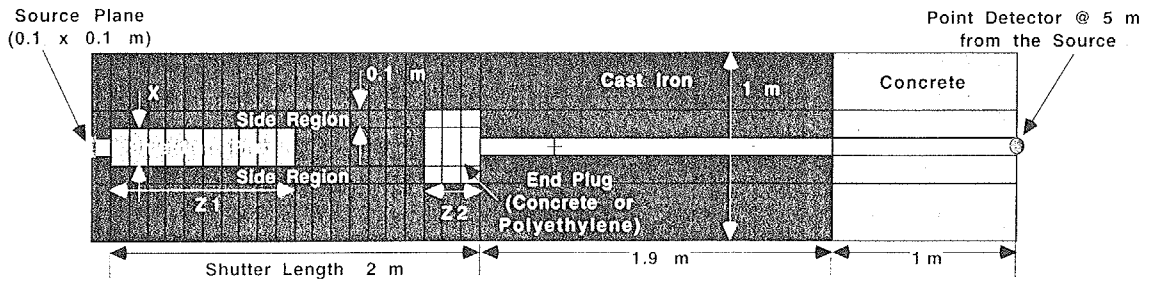

Fig. 10 Calculation model for optimizing the shutter configuration.

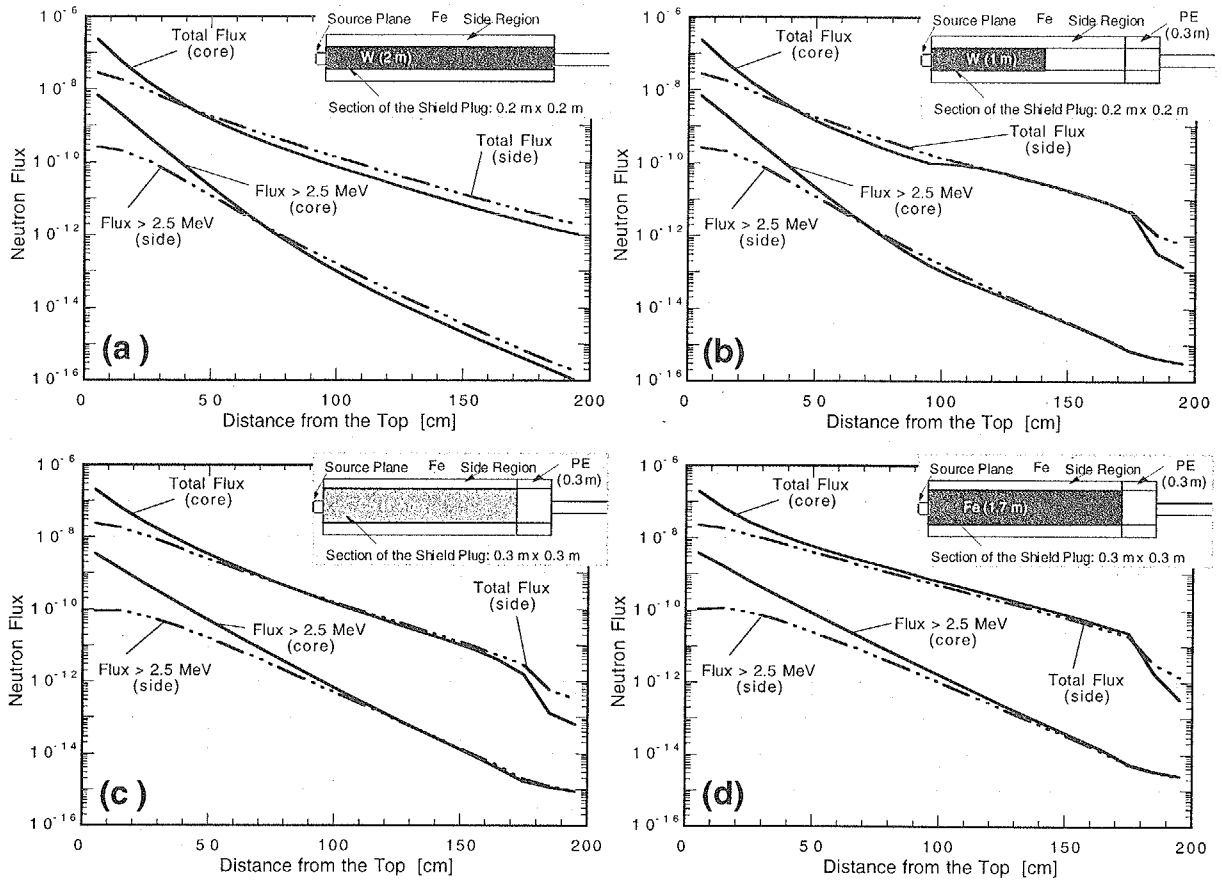

Fig. 11 Neutron flux distributions in the core and the side regions for the four types of shutter configurations.

region of iron is larger than that in the tungsten core region due to the large difference of the attenuation coefficients in the two materials. After the 1 m, high-energy neutron flux in the tungsten core region is dominated by the neutron flux leaking in the side region. This result indicates that it is not worth while extending the tungsten length more than ~ 1 m.

In the shutter (b), the length of tungsten is shortened to 1 m while an end plug of 0.3 m made of polyethylene is attached. Although the length of tungsten for the shutter (b) is a half of that for the shutter (a), differences in high-energy neutron fluxes at the end are not significant. On the contrary, the total neutron flux at the end for the shutter (b) is reduced by a factor of 10 compared to the shutter (a) due to the addition of the end plug.

In Figs. 11 (c) and (d), the shielding plug is replaced by copper and iron in the nominal density of 7.86 g/cm^3, respectively. As it is expected, the copper shutter (c) is superior to the iron shutter (d) for both high-energy and total neutron fluxes due to the higher weight density of copper compared to iron. The copper shutter (c) has nearly the same shielding performance as the tungsten shutter (b) although the copper shutter is much less expensive than the tungsten shutter. By taking account of the conclusion in the section 4.2, it can be concluded that the copper shutter is the most attractive in terms of shielding performance as well as cost merit.

4.4 Optimization for Beam Shutter Position

Figure 12 illustrates the weakest path for the beam line shielding starting from the target.

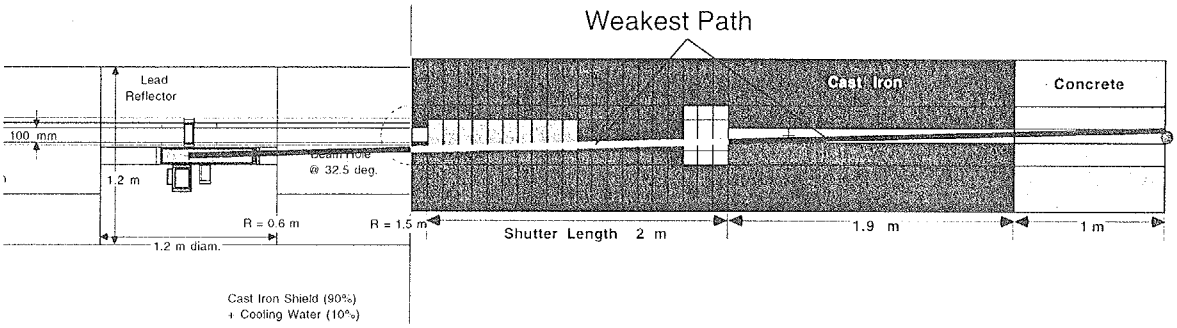

Fig. 12 The weakest path for the beam line shielding.

Although the overall thickness of bulk materials from the target center to the outside of the concrete shield is 6.5 m, neutrons from the target travel through the bulk shield of only 3.6 m thickness when they take the weakest path. One of ideas to ameliorate the difficulty is to move the shutter position outward. This movement, however, increases contribution of neutrons coming via the moderator. Accordingly, there must be an optimum position of the beam shutter at somewhere in the bulk shield. The beam shutter placed just outside the void vessel shown in Fig. 12 is not optimum from a view point of shielding. Investigation to find out the optimum position of the beam shutter is needed.

Summary

According to the shielding study, the following remarks were pointed out.

(1) Neutron dose outside of the concrete shield at 6.6 m from the center is ~ 10 μSv/hr regardless of angles with respect to the proton beam axis. The neutron dose can be reduced more than a factor of 30 by adding natural boron of 5 wt% in the concrete.

(2) When the beam shutter position just outside the void vessel and the shutter length of 2 m are assumed, a shutter made of copper (1.7 m) with polyethylene (0.3 m) is the optimum in terms of shielding performance as well as cost merit. A shutter made of tungsten is not so effective.

(3) Further studies are needed for optimization of beam shutter position.

Acknowledgment

The authors would like to express their sincere gratitude to staffs of the Information Systems Operating Division of the Center for Promotion of Computational Science and Engineering of JAERI for their efforts in developing the parallelized PC-cluster computer that enables us to perform a large amount of Monte Carlo simulation quickly.

References

[1] K. Niita, H. Takada, S. Meigo and Y. Ikeda, "High Energy Particle Transport Code NMTC/JAM", presented in this meeting.

[2] L. S. Waters (Ed.), "MCNPX™ User's Manual", TPO-E83-G-UG-X-00001, Los Alamos National Laboratory (1999).

[3] J. F. Briesmeister, (Ed.), "MCNP™ - A General Monte Carlo N-Particle Transport Code, Version 4C", LA-13709-M, Los Alamos National Laboratory, 2000.

[4] M. B. Chadwick, P. G. Young, S. Chiba, S. C. Frankle, G. M. Hale, H. G. Hughes, A. J. Koning, R. C. Little, R. E. MacFarlane, R. E. Prael, and L. S. Waters, "Cross Section Evaluations to 150 MeV for Accelerator-Driven Systems and Implementation in MCNPX", Nucl. Sci. Eng. **131** (1999) 293.